Plasticization of a Stiff Pharmaceutical Solid for Better Tabletability via Cocrystallization: Shape Synthons as Supramolecular Protecting Groups

Amit Mondal,^{a,\$} Biswajit Bhattacharya,^{a,\$} Hongbo Chen,^b Somayeh Khazaei,^c Susobhan Das,^a Surojit Bhunia,^a Somnath Dey,^a Rituparno Chowdhury,^a Manjima Bhattacharya,^a Alexandre Tkatchenko,^c Lewis L. Stevens,^d Changquan Calvin Sun,^{b,*} and C. Malla Reddy^{a,e*}

^aDepartment of Chemical Sciences, Indian Institute of Science Education and Research (IISER) Kolkata, Mohanpur Campus, Mohanpur, Nadia-741246, West Bengal, India.

^bDepartment of Pharmaceutics, University of Minnesota, Minneapolis, Minnesota 55455, United States.

^cDepartment of Physics and Materials Science, University of Luxembourg, L-1511 Luxembourg City, Luxembourg.

^dDepartment of Pharmaceutical Sciences and Experimental Therapeutics, University of Iowa, College of Pharmacy, Iowa City, IA 52241, United States.

^eDepartment of Chemistry, Indian institute of Technology Hyderabad, Kandi-502284, Sangareddy, Telangana, India

E-mail: sunx0053@umn.edu (CCS), cmallareddy@gmail.com (CMR)

ABSTRACT: Extremely high particle stiffness and very low hardness is a serious concern in various mechanical processes in pharmaceutical manufacturing. Here we report an exceptionally high Young's modulus (E) of \sim 18 GPa in a drug, isoniazid (INH). This is one of the highest experimentally determined values among all reported pharmaceutical molecular crystals, which we attribute to the presence of a strong three-dimensional (3D) hydrogen bonding network (HBN). Further, we successfully reduced the 3D HBN in INH to 2D in its cocrystal using a co-former, 3,4-dimethylbenzoic acid (DMBA), where its two hydrophobic groups act like protecting groups at supramolecular level and prevent the extension of HBN. This reduced the E in the 1:1 cocrystal, INH-DMBA, by many folds and markedly improved its powder tabletability. To the best of our knowledge, this is the first reliable molecular level

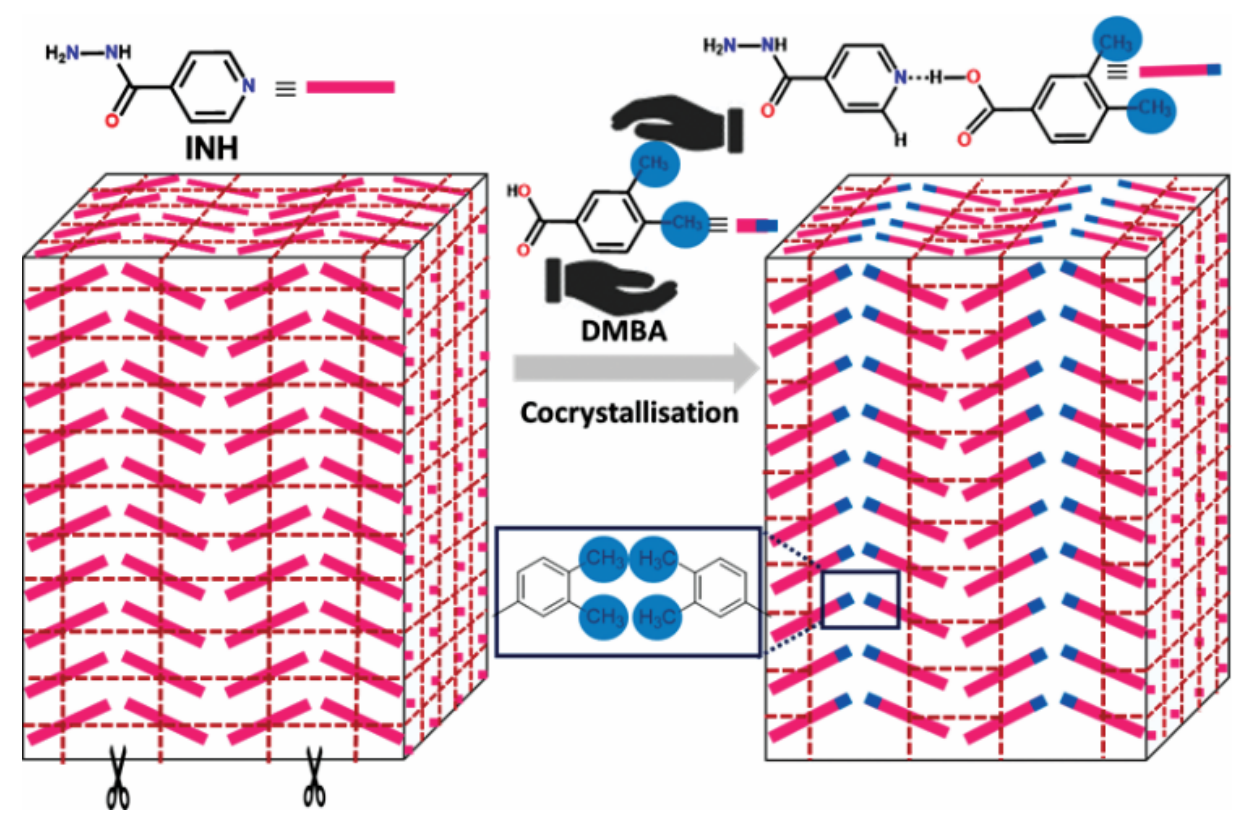
[§] Equal Contribution

approach to alter the stiffness of pharmaceutical crystals and tabletability improvement in a predictable manner, hence, is important in the context of crystal engineering.

Keywords: mechanical properties • stiffness • pharmaceutical drug • supramolecular synthons • tabletability

1. Introduction

Although the Young's modulus (E) of molecular crystals is shown to occupy a wide range from ~ 0.25 to ~ 45 GPa, most crystalline pharmaceutical solids, typically have a Young's modulus (E) in the range of 0.5 to 15 GPa. 1-5 Recent studies suggested that presence of strong hydrogen bonding networks could be one of the reasons for high mechanical stiffness in molecular crystals.³ Extremely high particle stiffness is undoubtedly an advantage in certain applications, but it can have adverse effects on various bulk powder processes in pharmaceutical industry. For instance, high stiffness may hinder powder compaction because of the low ability of particles to undergo permanent plastic deformation during compaction.⁶ Consequently, tablet mechanical strength is low due to the small inter-particulate bonding area in compressed tablets.⁷⁻¹³ This could be a serious concern in case of high dose tablets where the tabletability of active pharmaceutical ingredients (APIs) dominates that of the formulation. 14-16 Conversely, extremely high plasticity can lead to problems, such as punch sticking propensity and difficulty with milling.[17,18] Hence, one of the key challenges in pharmaceutical processing is to achieve optimum mechanical properties of the APIs. Recent studies attempted to link structure with mechanical behaviour of crystalline particles and the compaction of bulk powders.^[7-13, 19-35] In all co-crystal studies, the coformers were selected based on their ability to form co-crystals, but the ability to control tabletability of drug crystals, either increase or decrease, in a predictive manner has not been attained yet.



Scheme 1. Packing models showing the transformation of strong hydrogen bonded 3D network (left) in INH to 2D network (right) in the INH:DMBA cocrystal by using a supramolecular shape synthon approach, thus converting stiff solids to soft solids, respectively. Inset shows the Me···Me supramolecular shape synthon.

Here, we chose an important anti-tubercular drug, isoniazid (INH), as a model system for the tabletability problem of APIs (**Scheme 1**).^[36] The thick needle shaped crystals of INH, grown from ethanol, methanol or acetonitrile, are found to be brittle (Figure 1a) and hard due to presence of a strong 3D hydrogen bonding network (HBN) in its structure (**Figure 1b and 1c**).^[37] As a result, INH powders are unfit for direct compaction. Built upon recent progress in crystal engineering,^[3, 38-41] we hypothesised that the elimination of the strong 3D HBN by cocrystallization could be effective in improving crystal plasticity (**Scheme 1**) and, thus, tabletability. To test this hypothesis, we chose 3,4-dimethylbenzoic acid (DMBA) as a coformer, as it has two hydrophobic methyl (–Me) groups. The –Me groups used here prevent the extension of strong hydrogen bonding interactions in structure, hence can be considered as *supramolecular protecting groups*.

The acid group of DMBA binds with INH and blocks its hydrogen bonding sites from one side, while –Me groups close pack with themselves *via* soft supramolecular "shape

synthons" (i.e., geometrical shape driven, soft isotropic intermolecular interactions formed by weakly interacting hydrophobic or van der Waals (vdW) groups),^[38] to form slip planes (**Fig. 2**). Such slip planes can mediate slippage of molecules upon mechanical action, leading to higher plasticity and lower stiffness in crystals, as we show here. This report provides a unique molecular level approach to alter the stiffness of pharmaceutical crystals to improve tabletability in a predictable manner, which we achieved using soft supramolecular shape synthons *via* lowering the dimensionality of HBN.

2. Materials and methods

The API (INH) and the coformer (DMBA) were purchased from Sigma-Aldrich and commercially available solvents were used as received. Single component crystals of INH and DMBA were separately crystallized from ethanol by slow evaporation. The multicomponent crystal, INH-DMBA, was prepared by taking 1:1 molar ratio mixture of INH with DMBA using solvent assisted grinding with methanol, followed by slow evaporation from the same solvent. All the samples suitable for single crystal X-ray diffraction (SCXRD) and nanoindentation studies were obtained in 4–6 days. Further characterization was done using FT-IR (**Figure S1**), powder X-ray diffraction (PXRD, **Figure S2**) and differential scanning calorimetry (DSC, **Figure S3**). The structure-mechanical property correlation is investigated by well-established quantitative nanoindentation and powder compaction studies (see supporting information for experimental details).

3. Results and discussion

3.1. Crystal structure analysis of INH

The crystal structure of INH (P 2₁ 2₁ 2₁; Refcode: INICAC03)^[42-45] consists of hydrazide-hydrazide homosynthon through N–H···N (1.86 Å, 159°) and hydrazide-pyridine heterosynthon through N–H···N (1.95 Å, 170°) hydrogen bonds, resulting in a strong 3D network structure (**Figure 1b**). Energy frameworks analysis, which reveals the pairwise interaction energies among molecules in crystals, ^[46,47] also confirmed that the strong 3D hydrogen bonding network is the dominant feature in INH crystals (**Figures 1c and S4**).

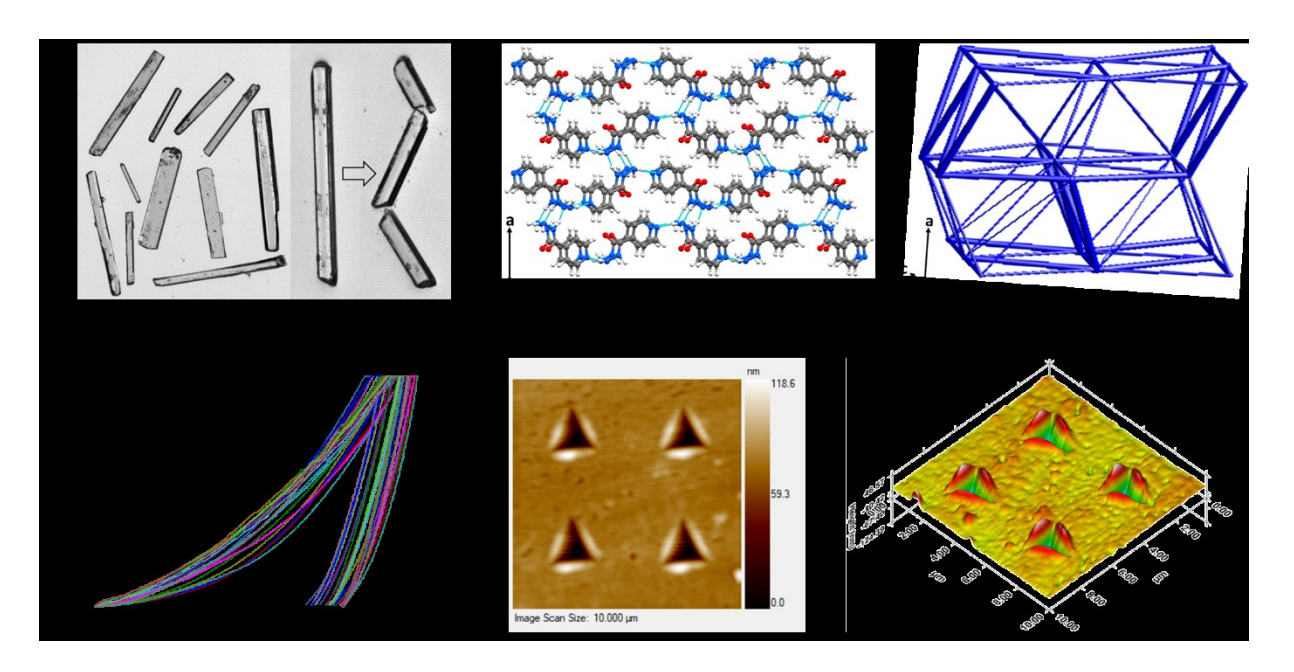


Figure 1. (a) Optical images of INH crystals and depiction of their brittle nature. (b) Strong interlocked 3D hydrogen bonded network in INH. (c) Energy frameworks skeleton showing the 3D nature of the packing (scale factor 25; energy threshold is 5 kJ mol⁻¹). (d) Nanoindentation load (P) - displacement (h) curves (with excellent repeatability) at 1mN load on (010) face. (e) 2D and (f) 3D impressions at 1mN load.

3.2. Quantification of mechanical properties of INH crystals

Although the crystals of INH, which grow in blocky rod type (or thick needle) morphologies, were found to be brittle and stiff from qualitative tests (**Figure 1a**), [11,37] quantitative assessment of mechanical properties of INH crystals was not done before. Therefore, we evaluated it both by experimental and computational techniques. We performed nanoindentation experiments on its major face (010) using a Berkovich diamond indenter tip of a radius 150 nm under load-controlled mode (see Supporting Information, face indexing, Figure S16). Typical load-displacement (P-h) curves and scanning probe microscopy (SPM) images of the indentation impressions from several single crystals are demonstrated in Figure 1d-f. Surprisingly, the measured elastic modulus, E, for (010) of INH was as high as 16.48 – 20.96 GPa while the hardness, H, was 0.44 – 0.87 GPa (**Figure 1d and Table 1**). We examined more than 25 crystals, each with several indents at different locations with smooth surface. The E and E and E values depended on the quality of the crystals, surface roughness and local defects. To eliminate any possible error in the measurement and to reconfirm such a high value, we have done the indentation experiments using both quasi-static and nano-DMA (dynamic mechanical analysis) methods for INH at 1 mN peak load and also at a higher load of 6 mN. The data

obtained from both the experiments show good repeatability with similar E and E and E values as discussed above (**Figure S9-S12, Table S6**). These exhaustive tests confirmed that the E value, ~ 18 GPa of INH on (010) is one of the highest among experimentally determined values for all pharmaceutical molecular crystals with known E, reported *hitherto*. The high E value of INH is also supported by both Brillouin light scattering (BLS) experiment and theoretical calculations (see supporting information for details).

The E of a material is the resistance exhibited by the indented material towards reversible elastic deformation and mechanical hardness is the resistance towards permanent plastic deformation. The high E observed in INH further supports recent suggestion that strong hydrogen bonding networks lead to high stiffness in molecular crystals [3, 37] due to their ability to act as shock-absorbers. The high E of INH is also consistent with the significant interaction energies in all directions obtained from energy frameworks analysis (**Figure 1c**). Having established the unprecedented stiffness in INH, we further used INH as a model system for tackling high stiffness issues in pharmaceutical drugs using cocrystallization.

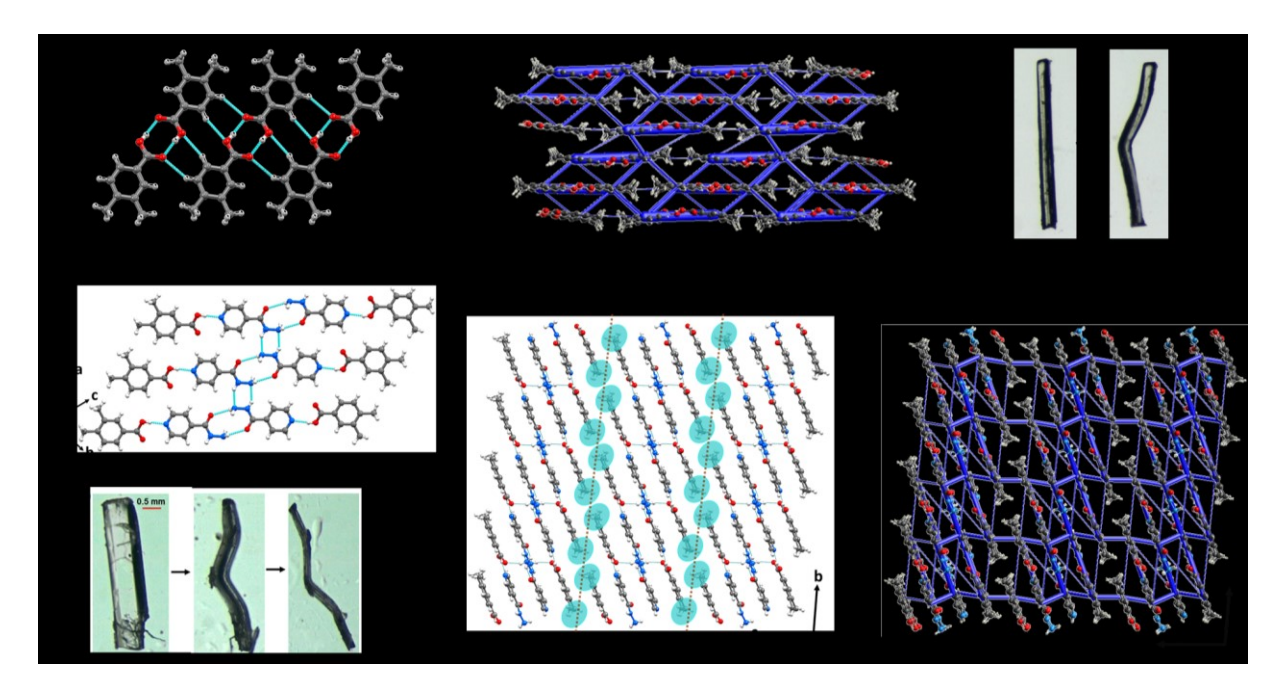


Figure 2. Crystal packing in the coformer, 3,4-dimethylbenzoic acid, DMBA showing (a) formation of 1D tape, (b) side view of layer like structure with energy frameworks (scale factor 25; energy threshold is 5 kJ mol⁻¹) and (c) plastic mechanical bending nature. Packing in the INH-DMBA cocrystal showing (d) hydrogen bonded tapes and (e) their further packing into 2D layer structure with slip planes. (f) Energy frameworks network and (g) qualitative plastic bending nature.

3.3. Crystal structure analysis of DMBA and INH-DMBA

Our SCXRD studies revealed that the rod-shaped crystals of DMBA adopt a triclinic space group *P*-1 (**Table S4**) with three molecules in the asymmetric unit. Overall packing is of flat layer type. DMBA molecules form acid dimers via strong O–H···O (1.81 Å, 171°) hydrogen bonds, which stack along *b*-axis to optimize the aromatic groups. Adjacent dimers interact via auxiliary C–H···O hydrogen bonds (2.6 Å, 147°; 2.54 Å, 155°) along *a*-axis (**Figure 2a**). In the third direction, *i.e.*, along *c*-axis, the molecules close pack via Me···Me shape synthons, which is in line with their expected dispersive nature. Energy frameworks analysis also confirmed that the plane formed by Me···Me is the weakest (**Figures 2b, S5 and S6**). Qualitative mechanical deformation tests revealed the plastic bending nature of the crystals on the major (001) face (**Figure 2c**).

Cocrystals of INH-DMBA grow as needles in the triclinic P-1 space group (**Table S4**) with one molecule of each INH and DMBA in the asymmetric unit. As strategized, the cocrystallization with DMBA successfully eliminates the 3D HBN in INH (Figures 2d,e). In the structure, two INH molecules interact with each other through head-to-head hydrazide···hydrazide homosynthon via N-H···O (2.29Å, 125°) and N-H···N (2.1 Å, 152°). Between the two additional N-H groups, one connects adjacent homosynthons while the second connects to the acid group of DMBA via a N-H···O in stacking direction. On the other hand, the pyridine group of INH binds to DMBA via acid-pyridine synthon (O-H···N: 1.7 Å, 175°). The two -Me groups on the terminal end of DMBA do not form any strong hydrogen bonds due to poor acidity of C–H. As a result, the HBN is not extended in that direction. These -Me groups with shape and interaction complementarity, playing a role of protecting groups in a supramolecular context, self-sort and close pack (Figure 2e). As a result, the hydrogen bonding in this structure is limited to 2D, rather than 3D in INH. Quantitative evaluation of intermolecular interactions by energy frameworks analysis revealed that the hydrogen bonded network contributes more to the structural stability than the slip plane parallel to (001) formed by the Me···Me groups (Figures 2f, S7 and S8). Qualitative three-point bending tests revealed that the cocrystal undergoes impressive plastic bending deformation (Figure 2g) on the (001) plane (major face). Note that the slip planes formed by Me...Me shape synthon shows in the structure are parallel to (001) plane (Figure 2e).

3.4. Quantitative assessment of mechanical properties and structure-mechanical property correlation

Though the mechanical bending experiments help quickly establish the deformation behavior of crystals, quantitative information is needed for distinguishing the crystals of a same class, and for more accurate prediction of bulk compaction properties. This is achieved through the well-established nanoindentation tests. The *P-h* curves from nanoindentation data show that, under the same load of 1 mN, the residual depth in the co-crystal INH-DMBA is considerably higher than that in parent INH crystals (**Figure 3 a, c, and S13-15**), indicating a significant improvement in its plasticity. This is confirmed by its significant lower *H* than INH (**Table 1**).

Compound	Indented facet	E (GPa)	H (GPa)
INH (Brittle)	(010)	$18.82 \ (\sigma \approx 1.25)$ $[16.48 - 20.96]$	$0.61 \ (\sigma \approx 0.13)$ $[0.44 - 0.87]$
DMBA (Plastically bendable)	(001)	$6.56 \ (\sigma \approx 0.28)$ $[5.82 - 6.99]$	$0.26 \ (\sigma \approx 0.01)$ [0.23 - 0.29]
INH-DMBA (Plastically bendable)	(001)	$6.9 \ (\sigma \approx 0.68)$ $[6.1 - 8.82]$	$0.41 \ (\sigma \approx 0.06)$ [0.3 - 0.5]

Table 1. Crystal mechanical properties quantified by nanoindentation at 1 mN load ($n \ge 25$).

The E showed a remarkable ~ 2.5 times decrease compared to that of INH crystals with respect to the major face (**Table 1**). Comparatively lower values of E and H in case of INH-DMBA than that of INH can be ascribed to the relatively softer intermolecular interactions resulting from 2D layer like structure separated by weak Me···Me shape synthons.

The E of the three crystals followed the descending order of INH > INH-DMBA > DMBA (**Table 1**). The pop-in features of the loading curves in DMBA and INH-DMBA indicate layer like structures and the response of slip planes during the indentation, which is generally observed in crystals undergoing shearing or plastic deformation (**Figure S13-14**). [48,49] Hence, the results obtained from nanoindentation analysis quantitatively confirm the significant decrease in the stiffness of the cocrystal compared to that of the parent INH crystal.

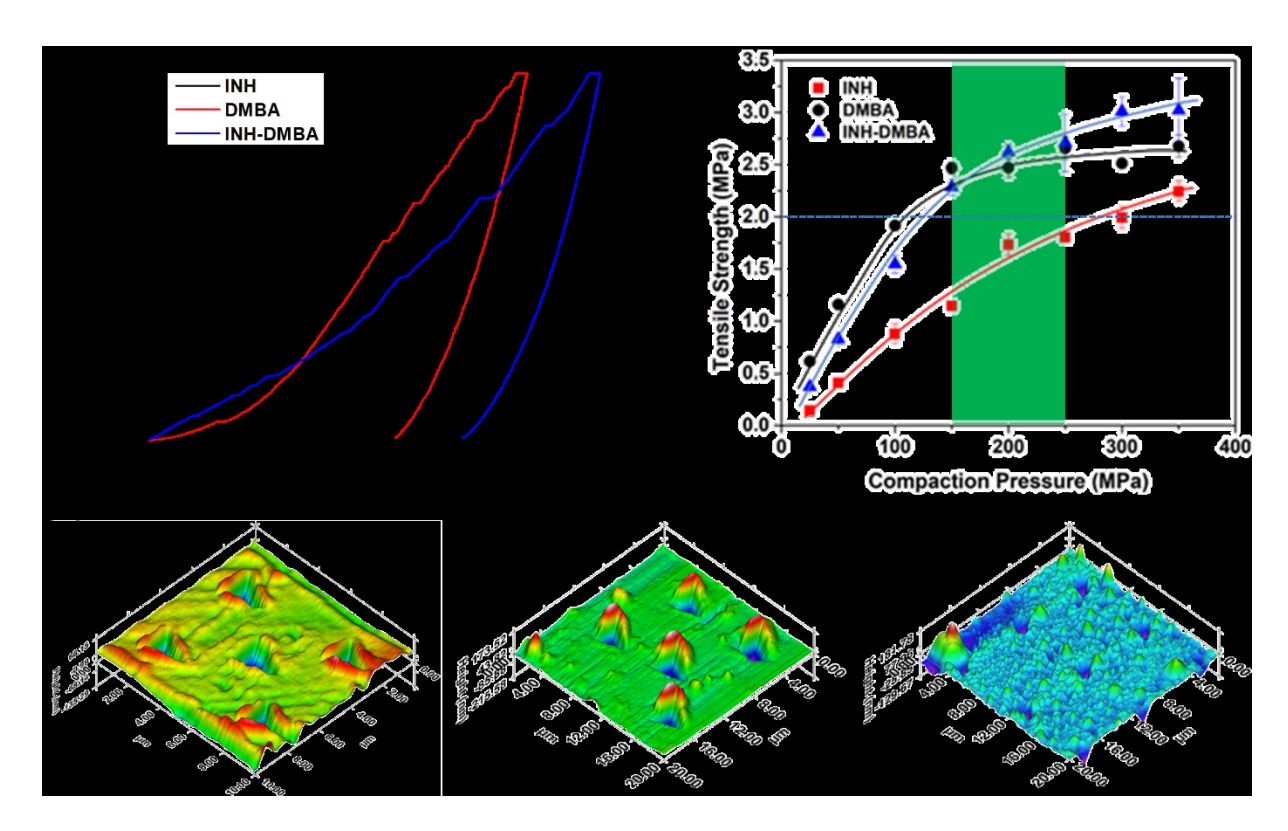


Figure 3. (a) Representative *P-h* curves for INH, DMBA and INH-DMBA. (b) Tabletability profiles of INH (red line), DMBA (black line) and INH-DMBA cocrystal (blue line). The desired tablet tensile strength of 2 MPa is shown as a horizontal dashed line and the desired compaction pressure zone is shown by the shaded area. (c) 3D indent impressions obtained from nanoindentation on crystals of INH, DMBA and INH-DMBA (from left to right, respectively).

3.5. Tabletability study

The improved plasticity of INH-DMBA cocrystal has a direct impact on tabletability. The desired tablet tensile strength for avoiding tableting problems is 2 MPa. [35] Tensile strength of INH increases nearly linearly with pressure and exceeds 2 MPa at about 300 MPa compaction pressure (**Figure 3b**). This is just outside the typical tabletability range as the desired compaction pressure normally varies between 150 – 250 MPa. In contrast, the more plastic DMBA and INH-DMBA formed tablets with 2 MPa tensile strength at about 100 MPa and 130 MPa, respectively (**Figure 3b**). The cocrystal is now well within typical pressure range in pharmaceutical tablet manufacturing. Thus, tableting performance of the INH-DMBA is significantly improved over INH.

4. Conclusion

In conclusion, here we report an exceptionally high stiffness of ~ 18 GPa in INH using nanoindentation and Brillouin light scattering measurements, supported by theoretical calculations. Presence of extensive strong hydrogen bonding network in INH leads to high stiffness. Hence, the INH crystals are found to be brittle and its bulk powder exhibits borderline tabletability. Note that the tabletability of INH would have been even poorer if the stiffness of all the faces was comparable to or higher than the (010) face (lower stiffness faces contribute more to deformation). Further, we successfully employed the crystal engineering approach to alter the 3D HBN crystal structure in INH to 2D network in the cocrystal by using the supramolecular shape synthons, much like the protecting groups used in organic synthesis. This allowed us to significantly reduce the stiffness and hardness in the cocrystal. As a result, the tabletability of the cocrystal was significantly improved. Thus, here we successfully showed that the crystal mechanical properties as well as tabletability of bulk APIs can be reliably modified using molecular level principles of crystal engineering. This study demonstrates that the soft supramolecular shape synthons can be effectively used for terminating strong hydrogen bonding networks in crystal structures, thus allowing manipulation of the dimensionality of HBN networks. The ability to manipulate mechanical properties through crystal structure engineering is particularly vital for designing various other dynamic crystalline materials, such as mechanochromic, luminescent, photosalient, thermosalient, and flexible optoelectronic, piezoelectric materials, etc. [52-72]

Acknowledgements

CMR thanks DST, New Delhi for Swarnajayanti Fellowship (DST/SJF/CSA-02/2014-15) and SERB for funding (No: CRG/2021/004992). Fellowships for BB (DST-SERB: PDF/2016/000262), AM (IISER-K), SuD (CSIR), SB (DST-INSPIRE), SoD (DST-SERB: PDF/2018/002502) and RC (KVPY, SX-1411075) are acknowledged. CCS thanks the National Science Foundation for support through the Industry University Collaborative Research Center (IUCRC) grant IIP-2137264, Center for Integrated Materials Science and Engineering for Pharmaceutical Products (CIMSEPP).

Conflicts of interest

There are no conflicts to declare.

References:

- Avinash, M. B.; Raut, D.; Mishra, M. K.; Ramamurty, U.; Govindaraju, T. Bioinspired Reductionistic Peptide Engineering for Exceptional Mechanical Properties. *Sci. Rep.* 2015, 5, 1-8.
- 2. Ramos, K. J.; Bahr, D. F. Mechanical Behavior Assessment of Sucrose Using Nanoindentation. *J. Mater. Res.* **2007**, *22*, 2037 2045.
- 3. Azuri, I.; Meirzadeh, E.; Ehre, D.; Cohen, S. R.; Rappe, A. M.; Lahav, M.; Lubomirsky, I.; Kronik, L. Unusually Large Young's Moduli of Amino Acid Molecular Crystals. *Angew. Chem. Int. Ed.* **2015**, *54*, 13566-13570.
- 4. Wang, C.; Sun, C. C. The landscape of mechanical properties of molecular crystals. *CrystEngComm*, **2020**, *61*, e202113988.
- 5. Karothu, D. P.; Halabi J. M.; Ahmed E.; Ferreira R.; Spackman P. R.; Spackman M. A.; Naumov P. Global Analysis of the Mechanical Properties of Organic Crystals. *Angew. Chem. Int. Ed.* **2022**, *54*, 13566-13570.
- 6. Sun, C. C. Decoding Powder Tabletability: Roles of Particle Adhesion and Plasticity. *J. Adhes. Sci. Technol.* **2011**, *25*, 483-499.
- 7. Sun, C. C.; Kleinebudde, P. Mini Review: Mechanisms to the Loss of Tabletability by Dry Granulation. *Eur. J. Pharm. Biopharm.* **2016**, *106*, 9-14.
- 8. Sun, C. C. A Classification System for Tableting Behaviors of Binary Powder Mixtures. *Asian J. Pharm. Sci.* **2016**, *11*, 486-491.
- 9. Hirschberg, C.; Sun, C. C.; Rantanen, J. Analytical Method Development for Powder Characterization: Visualization of the Critical Drug Loading Affecting the Processability of a Formulation for Direct Compression *J. Pharm. Biomed, Anal.* **2016**, *128*, 462-468.
- 10. Patel, S.; Sun, C.C. Macroindentation Hardness Measurement—Modernization and Applications. *Int. J. Pharm.* **2016**, *506*, 262-267.
- 11. Reddy, C. M.; Krishna, G. R.; Ghosh, S. Mechanical Properties of Molecular Crystals—Applications to Crystal Engineering. *CrystEngComm*, **2010**, *12*, 2296-2314.
- 12. Yadav, J. A.; Khomane, K. S.; Modi, S. R.; Ugale, B.; Yadav, R. N.; Nagaraja, C. M.; Kumar, N.; Bansal, A. K. Correlating Single Crystal Structure, Nanomechanical, and Bulk Compaction Behavior of Febuxostat Polymorphs. *Mol. Pharm.* 2017, 14, 866-874.

- 13. Dave, V. S.; Chanda, M.; Sayles, M.; Popielarczyk, M.; Boyce, H.; Bompelliwar, S. K.; Bates, S.; Morris, K. R.; Haware, R. V. Correlation of Structural and Macroscopic Properties of Starches with Their Tabletability Using the SM2 Approach. *J. Pharm. Sci*, 2015, 104, 3870-3882.
- 14. Yeboah, F. O.; Chang, S. Y.; Sun. C. C. A Critical Examination of the Phenomenon of Bonding Area-Bonding Strength Interplay in Powder Tableting. *Pharm. Res.* **2016**, *33*, 1126-1132.
- 15. Wang, C.; Perumalla, S.; Lu, R.; Fang, J.; Sun, C. C. Sweet Berberine. *Cryst. Growth Des.* **2016**, *16*, 933-939.
- Ullah, M.; Hussain, I.; Sun, C.C. The Development of Carbamazepine-Succinic Acid Cocrystal Tablet Formulations with Improved in Vitro and in Vivo Performance. Drug Dev. *Ind. Pharm.* 2016, 42, 969-976.
- 17. Wang, C.; Paul S.; Sun D. J.; Lill S. O. N.; Sun C. C. Mitigating Punch Sticking Propensity of Celecoxib by Cocrystallization: An Integrated Computational and Experimental Approach. *Cryst. Growth Des.* **2020**, *20*, 4217-4223.
- 18. Paul, S.; Wang, K.; Taylor, L. J.; Murphy, B.; Krzyzaniak, J.; Dawson, N.; Mullarney, M. P.; Meenan, P.; Sun, C. C. Dependence of punch sticking on compaction pressure—roles of particle deformability and tablet tensile strength. *Journal of Pharmaceutical Sciences*, **2017**, *106*, 2060-2067.
- 19. Ghosh, S.; Reddy, C. M. Elastic and Bendable Caffeine Cocrystals: Implications for the Design of Flexible Organic Materials. *Angew. Chem.* **2012**, *124*, 10465–10469.
- 20. Saha, S.; Mishra, M. K.; Reddy, C. M.; Desiraju, G. R. From Molecules to Interactions to Crystal Engineering: Mechanical Properties of Organic Solids. *Acc. Chem. Res.* **2018**, *51*, 2957–2967.
- 21. Saha, S.; Desiraju, G. R. Crystal Engineering of Hand-Twisted Helical Crystals. *J. Am. Chem. Soc.* **2017**, *139*, 1975-1983.
- 22. Takamizawa, S.; Miyamoto, Y. Superelastic Organic Crystals. *Angew. Chem., Int. Ed.* **2014**, *53*, 6970-6973.
- 23. Hayashi, S.; Yamamoto, S.-y.; Takeuchi, D.; Ie, Y.; Takagi, K. Creating Elastic Organic Crystals of π-Conjugated Molecules with Bending Mechanofluorochromism and Flexible Optical Waveguide. *Angew. Chem., Int. Ed.* **2018**, *57*, 17002-17008.
- 24. Panda, M. K.; Ghosh, S.; Yasuda, N.; Moriwaki, T.; Mukherjee, G. D.; Reddy, C. M.; Naumov, P. Spatially Resolved Analysis of Short-Range Structure Perturbations in a Plastically Bent Molecular Crystal. *Nat. Chem*, **2015**, *7*, 65-72.

- 25. Rupasinghe, T. P.; Hutchins, K. M.; Bandaranayake, B. S.; Ghorai, S.; Karunatilake, C.; Bucar, D.-K.; Swenson, D. C.; Arnold, M. A.; MacGillivray, L. R.; Tivanski, A. V. Mechanical Properties of a Series of Macro-and Nanodimensional Organic Cocrystals Correlate with Atomic Polarizability. J. Am. Chem. Soc. 2015, 137, 12768-12771.
- 26. Đakovic, M.; Borovina, M.; Pisac ič, M.; Aakero y, C. B.; Soldin, Ž.; Kukove, B. M.; Kodrin, I. Mechanically Responsive Crystalline Coordination Polymers with Controllable Elasticity. *Angew. Chem., Int. Ed.* **2018**, *57*, 14801-14805.
- 27. Worthy, A.; Grosjean, A.; Pfrunder, M. C.; Xu, Y.; Yan, C.; Edwards, G.; Clegg, J. K.; McMurtrie, J. C. Atomic Resolution of Structural Changes in Elastic Crystals of Copper(II) Acetylacetonate. *Nat. Chem.* 2018, 10, 65–69.
- 28. Huang, R.; Wang, C.; Wang, Y.; Zhang, H. Elastic Self-Doping Organic Single Crystals Exhibiting Flexible Optical Waveguide and Amplified Spontaneous Emission. *Adv. Mater.* **2018**, *30*, 1800814.
- 29. Rather, S. A.; Saha, B. K. Thermal Expansion Study as a Tool to Understand the Bending Mechanism in a Crystal. *Cryst. Growth Des*, **2018**, *18*, 2712-2716.
- 30. Wang, K.; Mishra, M. K.; Sun, C. C. An Exceptionally Elastic Single Component Pharmaceutical Crystal. *Chem. Mater.* **2019**, *31*, 1794-1799.
- 31. Sun, C. C.; Hou, H. Improving Mechanical Properties of Caffeine and Methyl Gallate Crystals by Cocrystallization. *Cryst. Growth Des.* **2008**, *8*, 1575-1579.
- 32. Bag, P. P.; Chen, M.; Sun, C. C.; Reddy, C. M. Direct Correlation Among Crystal Structure, Mechanical Behaviour and Tabletability in a Trimorphic Molecular Compound. *CrystEngComm*, **2012**, *14*, 3865-3867.
- 33. Karki, S.; Friščić, T.; Fábián, L.; Laity, P. R.; Day, G. M.; Jones, W. Improving Mechanical Properties of Crystalline Solids by Cocrystal Formation: New Compressible Forms of Paracetamol. *Adv. Mater.* **2009**, *21*, 3905–3909.
- 34. Krishna, G. R.; Shi, L.; Bag, P. P.; Sun, C. C.; Reddy, C. M. Correlation Among Crystal Structure, Mechanical Behavior, and Tabletability in the Co-crystals of Vanillin Isomers. *Cryst. Growth Des.* **2015**, *15*, 1827-1832.
- 35. Liu, L.; Wang, C.; Dun, J.; Chow, A. H. L.; Sun, C.C. Lack of Dependence of Mechanical Properties of Baicalein Cocrystals on Those of the Constituent Components. *CrystEngComm*, **2018**, *20*, 5486 5489.
- 36. World Health Organization (WHO) report **2013**, http://www.who.int/tb/publications/factsheet_global.pdf.

- 37. Reddy, C. M.; Padmanabhan, K. A.; Desiraju, G. R. Structure– Property Correlations in Bending and Brittle Organic Crystals. *Cryst. Growth Des.* **2006**, *6*, 2720-2731.
- 38. Krishna, G. R.; Devarapalli, R.; Lal, G.; Reddy, C. M. Mechanically Flexible Organic Crystals Achieved by Introducing Weak Interactions in Structure: Supramolecular Shape Synthons. *J. Am. Chem. Soc.* **2016**, *138*, 13561–13567.
- 39. Krishna, G. R.; Kiran, M. S. R. N.; Fraser, C. L.; Ramamurty, U.; Reddy, C. M. The Relationship of Solid-State Plasticity to Mechanochromic Luminescence in Difluoroboron Avobenzone Polymorphs. *Adv. Funct. Mater.* **2013**, *23*, 1422–1430.
- 40. Krishna, G. R.; Devarapalli, R.; Prusty, R.; Liu, T.; Fraser, C. L.; Ramamurty, U.; Reddy, C. M. Structure–Mechanical Property Correlations in Mechanochromic Luminescent Crystals of Boron Difluoride Dibenzoylmethane Derivatives. *IUCrJ*, **2015**, *2*, 611-619.
- 41. Raju, K. B.; Ranjan, S.; Vishnu, V. S.; Bhattacharya, M.; Bhattacharya, B.; Mukhopadhyay, A. K.; Reddy, C. M. Rationalizing Distinct Mechanical Properties of Three Polymorphs of a Drug Adduct by Nanoindentation and Energy Frameworks Analysis: Role of Slip Layer Topology and Weak Interactions. *Cryst. Growth Des.* 2018, 18, 3927-3937.
- 42. Jensen, L.H. The Crystal Structure of Isonicotinic Acid Hydrazide. *J. Am. Chem. Soc*, **1954**, *76*, 4663-4667.
- 43. Rajalakshmi, G.; Hathwarb, V. R.; Kumaradhasa, P. Topological Analysis of Electron Density and the Electrostatic Properties of Isoniazid: an Experimental and Theoretical Study. *Acta Cryst.* **2014**, *B70*, 331–341.
- 44. Lemmerer, A. Covalent Assistance to Supramolecular Synthesis: Modifying the Drug Functionality of the Antituberculosis API Isoniazid in Situ During Co-crystallization with GRAS and API Ccompounds. *CrystEngComm.* **2012**, *14*, 2465.
- 45. Bhat, T. N.; Singh, T.P.; Vijayan, M. Isonicotinic Acid Hydrazide–a Reinvestigation. *Acta Cryst.* **1974**, *B30*, 2921.
- 46. M. J. Turner, S. P. Thomas, M. W. Shi, D. Jayatilaka, M. A. Spackman. Energy Frameworks: Insights Into Interaction Anisotropy and the Mechanical Properties of Molecular Crystals. Chem. Commun. 2015, 51, 3735-3738.
- 47. Mackenzie, C. F.; Spackman, P. R.; Jayatilaka, D.; Spackman, M. A. CrystalExplorer Model Energies and Energy Frameworks: Extension to Metal Coordination Compounds, Organic Salts, Solvates and Open-Shell Systems. *IUCrJ*, **2017**, *4*, 575-587.

- 48. Varughese, S.; Kiran, M.; Ramamurty, U.; Desiraju, G. R. Nanoindentation in Crystal Engineering: Quantifying Mechanical Properties of Molecular Crystals. *Angew. Chem. Int. Ed.* **2013**, *52*, 2701-2712.
- 49. Kiran, M.; Varughese, S.; Reddy, C. M.; Ramamurty, U.; Desiraju, G. R. Mechanical Anisotropy in Crystalline Saccharin: Nanoindentation Studies. *Cryst. Growth Des.* **2010**, *10*, 4650-4655.
- 50. Garai, M.; Biradha, K. Coordination Polymers of Organic Polymers Synthesized via Photopolymerization of Single Crystals: Two-Dimensional Hydrogen Bonding Layers with Amazing Shock Absorbing Nature. *Chem. Commun*, **2014**, *50*, 3568-3570.
- 51. Garai, M.; Santra, R.; Biradha, K. Tunable Plastic Films of a Crystalline Polymer by Single-Crystal-to-Single-Crystal Photopolymerization of a Diene: Self-Templating and Shock-Absorbing Two-Dimensional Hydrogen-Bonding Layers. *Angew. Chem., Int. Ed*, **2013**, *52*, 5548-5551.
- 52. Naumov, P.; Chizhik, S.; Panda, M. K.; Nath, N. K.; Boldyreva, E. Mechanically Responsive Molecular Crystals. *Chem. Rev.* **2015**, *115*, 12440.
- 53. Kahr, B.; Ward, M. D. Stressed out crystals. *Nat. Chem.* **2017**, *10*, 4–6.
- 54. Zhu, L.; Al-Kaysi, R. O.; Bardeen, C. J. Photoinduced Ratchet-Like Rotational Motion of Branched Molecular Crystals. *Angew. Chem., Int. Ed.* **2016**, *55*, 7073-7076.
- 55. Devarapalli, R.; Kadambi, S. B.; Chen, C. T.; Krishna, G. R.; Kammari, B. R.; Buehler, M. J.; Ramamurty, U.; Reddy, C. M. Remarkably Distinct Mechanical Flexibility in Three Structurally Similar Semiconducting Organic Crystals Studied by Nanoindentation and Molecular Dynamics. *Chem. Mater.* 2019, 31, 1391-1402.
- 56. Hossain, M. S.; Ghosh, M.; Mondal, A.; Ajmal, P.; Saha, M.; Reddy, C. M.; Kurungot, S.; Bandyopadhyay, S. Water-chain mediated proton conductivity in mechanically flexible redox-active organic single crystals. *J. Mater. Chem. A*, **2024**, *12*, 5866-5874.
- 57. Ravi, J., Feiler, T., Mondal, A., Michalchuk, A. A., Reddy, C. M., Bhattacharya, B., ... & Chandrasekar, R. Plastically Bendable Organic Crystals for Monolithic and Hybrid Micro-Optical Circuits. *Advanced optical materials*, **2023**, *11*, 2201518.
- 58. Samanta, R., Das, S., Mondal, S., Alkhidir, T., Mohamed, S., Senanayak, S. P., & Reddy, C. M. Elastic organic semiconducting single crystals for durable all-flexible field-effect transistors: insights into the bending mechanism. *Chemical Science*, 2023, 14, 1363-1371.

- 59. Das, S., Saha, S., Sahu, M., Mondal, A., & Reddy, C. M. Temperature-reliant dynamic properties and elasto-plastic to plastic crystal (rotator) phase transition in a metal oxyacid salt. *Angewandte Chemie*, **2022**, *134*, e202115359.
- 60. Mondal, A., Bhattacharya, B., Das, S., Bhunia, S., Chowdhury, R., Dey, S., & Reddy, C. M. Metal-like Ductility in Organic Plastic Crystals: Role of Molecular Shape and Dihydrogen Bonding Interactions in Aminoboranes. *Angewandte Chemie International Edition*, 2020, 59, 10971-10980.
- Annadhasan, M., Agrawal, A. R., Bhunia, S., Pradeep, V. V., Zade, S. S., Reddy, C. M., & Chandrasekar, R. Mechanophotonics: Flexible single-crystal organic waveguides and circuits. *Angewandte Chemie*, 2020, 132, 13956-13962.
- 62. Das, S., Mondal, A., & Reddy, C. M. Harnessing molecular rotations in plastic crystals: a holistic view for crystal engineering of adaptive soft materials. *Chemical Society Reviews*, **2020**, *49*, 8878-8896.
- 63. Bhunia, S., Chandel, S., Karan, S. K., Dey, S., Tiwari, A., Das, S., ... & Reddy, C. M. Autonomous self-repair in piezoelectric molecular crystals. *Science*, **2021**, *373*, 321-327.
- 64. Mondal, S., Tanari, P., Roy, S., Bhunia, S., Chowdhury, R., Pal, A. K., ... & Reddy, C.
 M. Autonomous self-healing organic crystals for nonlinear optics. *Nature Communications*, 2023, 14, 6589.
- 65. Ahmed, E., Karothu, D. P., & Naumov, P. Crystal adaptronics: mechanically reconfigurable elastic and superelastic molecular crystals. *Angewandte Chemie International Edition*, **2018**, *57*, 8837-8846.
- 66. Bhunia, S.; Karan, S. K.; Chowdhury, R.; Ghosh, I.; Saha, S.; Das, K.; Mondal, A.; Nanda, A.; Khatua, B. B.; Reddy, C. M. Mechanically flexible piezoelectric organic single crystals for electrical energy harvesting, *Chem*, **2024**, *Just accepted*. DOI: https://doi.org/10.1016/j.chempr.2024.01.019.
- 67. Awad, W. M., Davies, D. W., Kitagawa, D., Halabi, J. M., Al-Handawi, M. B., Tahir, I., ... & Naumov, P. Mechanical properties and peculiarities of molecular crystals. *Chem. Soc. Rev.*, **2023**, *52*, 3098–3169.
- 68. Deka, P., Das, S., Sarma, P., Kalita, K. J., Vijayaraghavan, R. K., Reddy, C. M. & Thakuria R. Exceptional Thermo-Mechano-Fluorochromism and Nanomechanical Analysis of Mechanically Responsive J and H Type Polymorphic Systems. *Cryst. Growth Des.* **2024**, *24*, 2322–2330.

- 69. Hazarika, P. J., Gupta P., Gunnam, A., Thakuria, R., Nangia, A. K. & Nath, N. K. Flexible Chlorinated Azine Molecular Crystals and Their Photothermally Driven Actuation. *Cryst. Growth Des.* **2024**, *24*, 763–773.
- 70. Mishra, M. K., Mishra, K., Narayan, A., Reddy, C. M., & Vangala, V. R. Structural basis for mechanical anisotropy in polymorphs of a caffeine–glutaric acid cocrystal. *Crystal Growth & Design*, **2020**, *20*, 6306-6315.
- 71. Yousef, M. A. E. & Vangala, V. R. Pharmaceutical Cocrystals: Molecules, Crystals, Formulations, Medicines. *Cryst. Growth Des.* **2019**, *19*, 7420–7438.
- 72. Zhang, K., Fellah, N., Shtukenberg, A. G., Fu, X., Hu, C., & Ward, M. D. Discovery of new polymorphs of the tuberculosis drug isoniazid. *CrystEngComm*, **2020**, *22*, 2705-2708.